Journal of Chromatography B, 905 (2012) 43–53

Contents lists available at SciVerse ScienceDirect

Journal of Chromatography B

journal homepage: www.elsevier.com/locate/chromb

Post acquisition data processing techniques for lipid analysis by quadrupole time-of-flight mass spectrometry

Tong Xie[1], Yan Liang**,[1], Jiye A, Haiping Hao, Linsheng Liu, Xiao Zheng, Chen Dai, Yuanyuan Zhou, Tianye Guan, Yanna Liu, Lin Xie, Guangji Wang*

State Key Laboratory of Natural Medicines, Key Lab of Drug Metabolism & Pharmacokinetics, China Pharmaceutical University, Tongjiaxiang 24, Nanjing 210009, China

ARTICLE INFO

Article history:
Received 8 March 2012
Accepted 1 August 2012
Available online 9 August 2012

Keywords:
Lipid detection
LCMS-Q-TOF
Product ion filtration
Neutral loss filtration
Mass defect filtration

ABSTRACT

This study describes the effectiveness of post-acquisition data processing techniques in detecting the lipid species rapidly from the massive data generated by high resolution mass spectrometry. The filtering approaches by product ions or neutral losses enabled glycerophospholipids and sterol conjugates to be identified based on the investigation of their fragmentation patterns, and the filtration by mass defect facilitated the detection of fatty acyl residues and bile acids by limiting the range of mass defect values. After application of these filtering techniques to mass spectra, the background noise was significantly filtered out and characteristic peaks of lipid species were efficiently sorted out. Totally 145 individual lipids were identified and structurally elucidated. Validation results of the LCMS-Q-TOF-based quantitative performance for all the peaks showed that the accuracy, expressed as relative errors (RE%), was lower than ±15%, and values (RSD%) of the inter-batch and intra-batch precision were lower than 15% in the assay. The developed method was integrated to the evaluation of plasma lipid profile from high fat diet versus energy restricted diet fed rats. A unique discrimination of the groups was successfully achieved through a principal component analysis (PCA).

© 2012 Published by Elsevier B.V.

1. Introduction

High resolution mass spectrometry has become an important tool in the qualitative and quantitative analysis of multiple compounds in complex matrices including herbal components [1,2], endogenous metabolites [3], peptides [4], and lipids [5]. However, a great challenge normally encountered in data processing is the detection of untargeted components as the ions of potential interest are largely masked by background noise. To address this problem, several post acquisition data processing techniques have been developed to facilitate the spectrum analysis, such as isotope filtering method and background subtraction approach [6–8]. In addition, extraction of target ions by fragment ion, neutral loss or mass defect was frequently adopted to screen potential drug metabolites in biological samples [9] or facilitate multi-component analysis from complex systems such as herbal extracts [10]. Integration of these methods has proven valuable in improving the robustness, automation, and ease of the data mining process. Nevertheless, innovation of post data processing strategy in terms of accuracy, completeness, and efficiency to provide maximum information is still an active research direction.

Lipids comprise an extremely heterogeneous collection of molecules from a structural and functional standpoint. A large number of studies have critically linked disease pathology to the disruption of lipid metabolic pathways [11,12]. The ever growing interest in their pathophysiological roles conceivably puts a high demand on analytical strategies that enable a global insight into diverse lipids from biological samples. In this regard, a triple quadrupole mass spectrometry-based method, defined as 'shotgun lipidomics,' could be employed to achieve lipid detection through neutral losses or precursor ion scannings after direct MS infusion without prior chromatographic separation [11,12]. Han et al. extensively reviewed the principles of this shotgun lipidomics to select specific precursor ions or neutral losses for the detection of various lipid species [11,13]. Recently, Shevchenko et al. reported the lipid profiling by multiple precursor and neutral loss scanning with the combined use of hybrid quadrupole time-of-flight mass spectrometers and a robotic nano-flow ion source. Obviously, their automated data-dependent acquisition enabled the emulation of precursor and neutral loss scans in a single analysis [14], but, a typical limitation was the presence of ion suppression and the problem in effectively quantifying hundreds of distinct species. Additionally, the systematic use of multiple precursor ion or neutral loss

* Corresponding author. Tel.: +86 2583271128; fax: +86 2583302827.
** Corresponding author. Tel.: +86 2583271179; fax: +86 2583271060.
E-mail addresses: liangyan@cpu.edu.cn, cpuly0679@yahoo.cn (Y. Liang), guangjiwang@hotmail.com (G. Wang).
[1] These authors contributed equally to this work.

1570-0232/$ – see front matter © 2012 Published by Elsevier B.V.
http://dx.doi.org/10.1016/j.jchromb.2012.08.001

scanning should put restrictions on certain molecules that cannot be fragmented in collision cell using the defined collision energy.

To address the problems, we used liquid chromatography hybrid quadrupole time-of-flight mass spectrometer (LCMS-Q-TOF) to acquire the full scan data. As the chromatographic separation was used, quantitative analysis for lipid species can be accurately evaluated. In this study, we studied the MS/MS fragmentation of lipid species to trigger the fragment ion and neutral loss filtration. To detecting lipid species which are inaccessible to fragmentation, mass defect filtration was introduced as a complementary method. Herein, mass defect of an element is defined as the residual mass of the exact mass and nominal mass and mass defect of a compound or an ion could be obtained by summarizing the mass defects of its elemental constituents. Theoretically, mass defect of compounds with common substructures changes in a limited range. The mass defect is highly the characteristic of constituent atoms and is useful in data handling. According to imaging the mass defect ranges, the distinct lipid species can be segregated. Furthermore, to demonstrate the utility of this method, we have applied it to biological samples from high fat diet (HFD) and energy restricted diet (ERD) fed rats, and show that it can effectively identify the differential lipid features.

2. Materials and methods

2.1. Chemicals, regents, and materials

Cholic acid, chenodeoxycholic acid, deoxycholic acid, lithocholic acid, dehydrocholic acid, glycocholic acid, chenodeoxycholic acid glycine conjugate, diazepam, and rheinic acid were ordered from Sigma–Aldrich (St. Louis, MO, USA). Acetonitrile of HPLC grade was purchased from Sigma–Aldrich (St. Louis, MO, USA), and was used to prepare the solutions of lipids.

2.2. Chromatographic and mass spectrometric conditions

Lipid analysis was performed on a Shimadzu 30A system (Shimadzu Corporation, Kyoto, Japan) with a SIL-30A autosampler, a CTO-20A column oven and an LC-30A binary pump. For each run, a sample volume of 5 μL was injected onto a Phenomenex Luna C_{18} (150 mm × 2.1 mm, 5 μm) at a flow rate of 200 μL/min, with a total run time of 65 min. A linear gradient elution was used, consisting of solvent A (containing 0.02% formic acid in water) and solvent B (containing 0.02% formic acid in acetonitrile). To achieve a better separation, the gradient was initially maintained at 10% B for 2 min, ramped to 50% in 10 min, ramped to 95% B in 50 min, held for 5 min at 95%, and then returned to 10% for next 8 min.

Lipids were analyzed in negative and positive ion modes on a hybrid quadrupole time-of-light mass spectrometer (LCMS-Q-TOF, Triple TOF 5600 system, Applied Biosystems/MDS Sciex, Comcord, ON, Canada) equipped with a Turbo V ion spray source. Ionization voltage was set to −5.5/4.5 kV (negative/positive) and spray temperature was maintained at 400 °C. Nebulizer gas and heater gas pressure was set to 50 psi and curtain gas pressure was to 30 psi. A typical information dependent acquisition consists of two steps: the acquisition of a survey TOF MS spectrum and then a MS/MS experiment. TOF MS scan was operated under the high resolution settings. The optimized declustering potential (DP) and collision energy (CE) were set at −120 eV and −10 eV in the negative ion mode, and at 120 eV and 10 eV in the positive ion mode. In the second experiment, product ion scan was acquired in 250 ms if precursor ions exceeded a threshold of 300 counts per second. A sweeping collision energy setting at −30/30 eV ± 15 eV was applied for collision-induced dissociation (CID). Continuous recalibration was carried out every 6 h by EasyMass Accuracy® device. All spectra were controlled by Analyst 1.5.1 of Applied Biosystems/MDS Sciex.

2.3. Sample collection and preparation

Male Sprague Dawley rats (weight: 180–220 g) were obtained from the Laboratory Animal Center of Peking University Health Science Center (Beijing, China). All the rats were acclimated for at least two weeks before the experiments and allowed water and fed with standard laboratory food. All animal studies were approved by the Animal Ethics Committee of China Pharmaceutical University. Rats were randomly divided into three groups with eight animals in each group. The control group received commercial nutritious mixtures. The high fat diet fed (HFD) rats received high fat diet containing 0.5% cholesterol and 10% lard. The energy restricted diet fed (ER) rats received 40% of daily intake of the control groups. The experiments were last for two weeks. After experiments, the venous blood was collected for lipid analysis.

For sample purification, 980 μL of methanol were added to 200 μL rat plasma sample. The mixture was spiked with 10 μL diazepam (2.0 μg/mL) and 10 μL rheinic acid (2.0 μg/mL) which were used to calibrate in the positive and negative ion mode. The sample was then vortexed 10 min, followed by centrifugation for 10 min at 18,000 rpm at room temperature. The supernatant was transferred into a new tube and evaporated to dryness in a rotary evaporator at 45 °C. The residue was reconstituted in 200 μL methanol and centrifuged at 40,000 × *g* for 10 min. A 5 μL aliquot was injected into the LCMS-Q-TOF system for analysis.

2.4. Data analysis

Endogenous interferences subtraction and lipid molecule screening from the raw data were processed by filtering methods. The filtering approaches were processed based on the principles; first, lipid species producing specific product ions or neutral loss in collision-induced dissociation (CID) were screened out by fragment ion filtration or neutral loss filtration; second, the molecules producing no fragments were detected by mass defect filtration.

Fragment ion or neutral loss filtration was automatically carried out based on setting criteria with a prototype script of IDA Trace Extractor written by Analyst 1.5.1 of Applied Biosystems/MDS Sciex. Ranges of *m*/*z* were employed into the chromatographic data to obtain the filtered chromatograms and lists containing *m*/*z* and retention time. Mass defect filtration was carried out by PeakView 1.1.1.2 (Applied Biosystems/MDS Sciex, Comcord, ON, Canada). According to a user-defined formula and mass defect tolerance, the filtered chromatograms and lists can be obtained. For next structural identification, the *m*/*z* and retention time were used to conduct extract ion chromatograms (EICs). All the detected *m*/*z* values were imported into the Human Metabolome Database (HMDB, http://www.hmdb.ca/) [15], the LIPID MAPs (http://www.lipidmaps.org/) [16], and Metlin Database (http://masspec.scripps.edu/) for structural characterization.

For quantification, automated retention time alignment and peak integration were implemented with MarkerView software 2.1 (Applied Biosystems/MDS Sciex, Comcord, ON, Canada). The produced data matrix containing peak index and their normalized peak response was submitted into the SIMCA-P software 11.0 (Umetrics, Umea, Sweden). The unsupervised principal component analysis (PCA) was employed to demonstrate general cluster and trends among the observations. Characterization of differential lipid features was performed using one-way ANOVA (SPSS 16.0) with a significance level of 0.05, and correction towards false positives was performed by Bonferroni.

3. Results and discussion

3.1. Product ion and neutral loss filtration

Mass spectra were recorded in the positive and negative ion modes to effectively highlight our LCMS-Q-TOF approach for coverage of total lipids [17]. The chromatographic conditions were optimized for sufficient separation of the isobaric and isomeric molecules. As illustrated in TICs (Figs. 1 and 2A), detection was severely challenged because the target ions were interfered by background signals. We employed filtering methods to remove the interferences and screen the characteristic peaks by analysis of their fragmentation patterns.

To validate the useful and powerful of the filtering methods, three species of lipid molecules in plasma samples were tested. First we applied fragment ion filtration and neutral loss filtration to detect glycerophospholipids including choline glycerophospholipids and ethanolamine glycerophospholipids in the raw data. Glycerophospholipids (GPs) are glycerol-based phospholipids which are the main components of biological membranes, consisting of a glycerol phosphate backbone with a headgroup attached at the *sn*-3 position and two fatty acyl moieties attached to the remaining two positions via ester or ether bonds. By collision induced dissociation (CID), fragmentation of polar head groups produced specific products or losses which can be used for detection [18].

Choline glycerophospholipids (PCs) are lipid molecules with a positively charged quaternary ammonium bounding to the phosphate. Because of the inherent amphoteric property, the EICs were detected as $[M+H]^+$ in the positive ion mode and $[M+HCOO]^-$ in the negative ion mode. MS/MS fragmentation of $[M+H]^+$ tended to produce two product ions at *m*/*z* 184.0733 $[C_5H_{15}NO_4P]^+$ and 104.1070 $[C_5H_{14}NO]^+$. The fragmentation of $[M+HCOO]^-$ in the negative ion mode lost the neutral fragments of 60.0813 Da ($C_3H_{10}N$) and 285.0977 Da ($C_7H_{16}NO_5P$) (Fig. 3A). In view of the high intensity, the fragment at *m*/*z* 184.0733 was defined as a probe to filter the PCs from the original data. Fragments between *m*/*z* 184.0633 and 184.0833 was employed into the TICs. The filtered chromatogram was automatically and rapidly obtained. From the filtered chromatogram (Fig. 1B), the peaks of the potential PCs were completely apparent. Extracted ion chromatographic analysis was employed to confirm them, and a total of 41 PCs were screen out (Table 1). Potential structural characterization with predicted formula (Error < 5 ppm) was achieved according to database searching. Although some false candidates were screened out, it was easy to exclude according to the database matching. By inspecting the separate EICs, we concluded that the co-eluting peaks were always revealed. These isomeric peaks should be attributed to the different positions of the fatty acyl chain. However, these isomers presented the similar MS/MS spectra, and we failed to distinguish them.

Ethanolamine glycerophospholipids (PEs) have a polar head group of phosphoethanolamine. In the positive ion mode, CID of the $[M+H]^+$ ions appeared to loss the phosphoethanolamine corresponding to 141.0191 Da ($C_2H_8NO_4P$). In the negative ion mode, PEs presented predominantly the $[M+HCOO]^-$ ions in the MS spectra and the neutral loss of 197.0453 Da ($C_5H_{12}NO_5P$) in the MS/MS spectra (Fig. 3B). Because of high intensity in the positive ion mode, characteristic neutral loss filtration from 141.0091 to 141.0291 Da was set to filter the PEs. The filtered chromatogram was illustrated in Fig. 1C and a total of 8 PEs were structurally identified (Table 1).

To further validate the performance of the filtering methods, glycine conjugates in the plasma samples were analyzed. Glycine conjugates of bile acids can be detected in the positive ion mode and produce the abundant product ions according to the previous literatures [19–21], while taurine conjugates and unconjugated bile acids are mainly detected in the negative ion mode and produce the limited product ions in the CID. Therefore, we conducted the product ion or neutral loss filtration method to detect the glycine conjugates. To get better understanding of the fragmental patterns of glycine conjugates, the representative authentic standards of glycocholic acid and chenodeoxycholic acid glycine were investigated. Taking glycocholic acid as an example for detailed characterization, the MS spectrum of the glycocholic acid in the positive ion mode was characterized by the $[M+H]^+$, $[M+NH_4]^+$, $[M+H-H_2O]^+$, $[M+H-2H_2O]^+$, and $[2M+H]^+$ ions. In the MS/MS spectrum, the $[M+H]^+$ ion (*m*/*z* 466.3169) was isolated to produce the ions at *m*/*z* 158.0888, 199.1576, 209.1424, 213.1736, 227.1542, 227.1904, 319.2567, 337.2677, 412.3034, 430.3142, and 448.3249. Clearly, the yielded ions at *m*/*z* 448.3249, 430.3142, and 412.3034 were derived from the $[M+H-H_2O]^+$, $[M+H-2H_2O]^+$, and $[M+H-3H_2O]^+$ ions (Fig. 4A). It was suggested that the MS/MS spectrum of the glycine conjugates were predominantly dominated by $[M+H-nH_2O]^+$, where "*n*" was the number of the hydroxyl groups in the structures. Additionally, the ions at *m*/*z* 337.2677 and 213.1736 were derived from the successive loss of acetamide and D-ring, producing the typical loss of 75.0320 Da ($C_2H_5NO_2$) and 124.0888 Da ($C_8H_{12}O$). The same fragmentation pathway was presented of chenodeoxycholic acid glycine (Fig. 4B). Because the lost moiety of $C_8H_{12}O$ (75.0320 Da) was the common substructure of glycine conjugates, we considered it as the filtration probe (Fig. 3B). We applied the neutral loss filtration of 75.0220–75.0420 Da into the raw data. The filtered chromatogram was illustrated in Fig. 1D and only eleven peaks were finally assigned for structural elucidation (Table 2). In our study, taurine conjugates were not detected in our study because the low concentration that could not be achieved in our study.

This filtration was then extended to the detection of the glucuronic acid conjugates. In the negative ion mode, the presence of the glucuronic acid moiety produced the neutral loss of 176.0321 Da ($C_6H_8O_6$) in MS/MS spectrum. Therefore, the neutral loss filtration from 176.0221 Da to 176.0421 Da was used to detect the glucuronic acid conjugates (Fig. 2B) and twenty-four peaks were detected (Table 2).

3.2. Mass defect filtration

Mass defect of an ion or molecule is the difference between their exact mass and nominal (integer) mass and it was highly the characteristic of constituent atoms. Spectrum filtration by mass defect was designed provided that there was a similarity in the mass defects among the species of interest and it can selectively remove the heterogeneous ions that fall outside of the filter window [8]. According to defining the mass defect ranges of the species, filtration of chromatograms can be easily achieved. Numerous literature had reported its practical application for detection of metabolites [9,10,22].

Each species of lipids have their distinct substructures and mass defect of these substructures can be used to distinguish them. In this study, we determined the mass defect ranges by the standard mass defect profiles depicted by all the published lipids in LIPID MAP database (http://www.lipidmaps.org/data/classification/LM_classification_exp.php) with the *m*/*z* on the *x-axis* and the mass defect on the *y-axis*. The mass defect filtration was then performed by the formula expressed as (central formula ± mass defect tolerance) in which central formula equals the half of maximum and minimum element constituent, and mass defect tolerance equals the half width of mass defects ranges. First, we took the detection of fatty acyls to show the applicable of the method.

The analysis of fatty acyls was complicated because of the structural diversity. Previous studies reported that the location of double bonds, alkyl substituents, and ring structures could

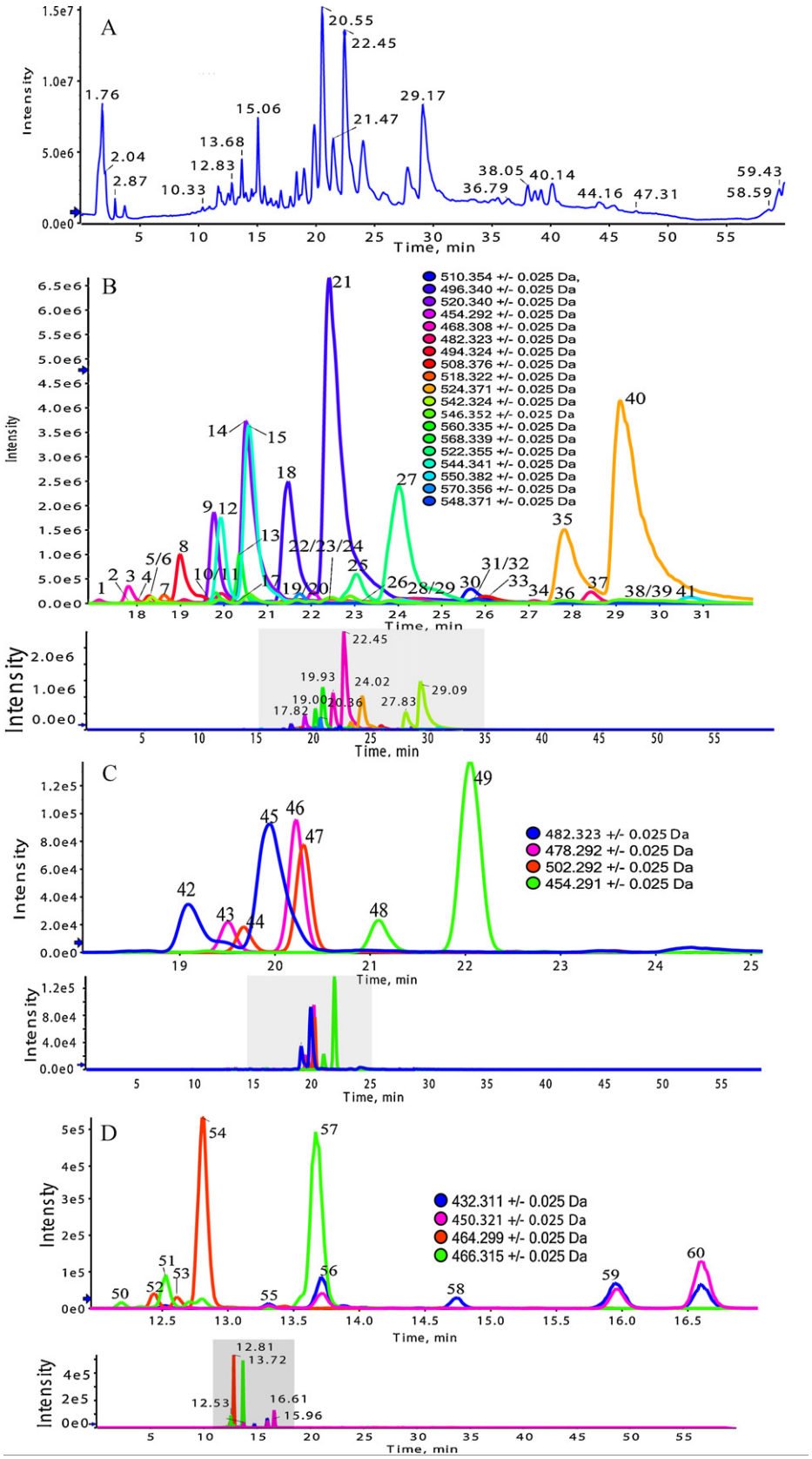

Fig. 1. (A) The unfiltered chromatogram determined in positive ion mode and (B) the filtered chromatogram of choline glycerophospholipids, (C) ethanolamine glycerophospholipids, and (D) glycine conjugates of bile acids detected by product ion or neutral loss filtration method.

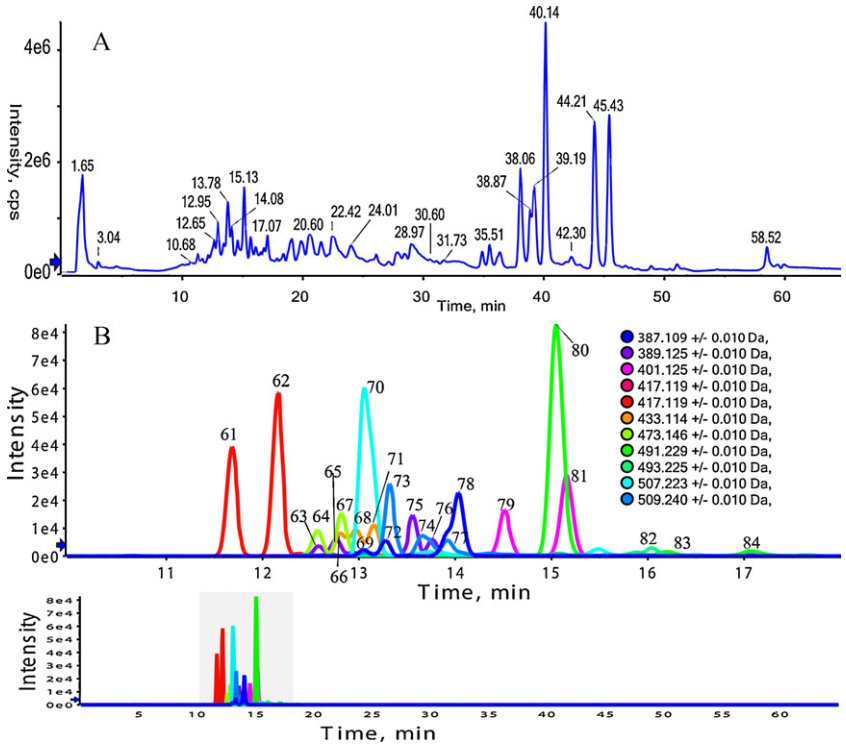

Fig. 2. (A) The unfiltered chromatogram determined in negative ion mode and (B) the filtered chromatogram of glucuronic acid conjunctions detected by product ion filtration method.

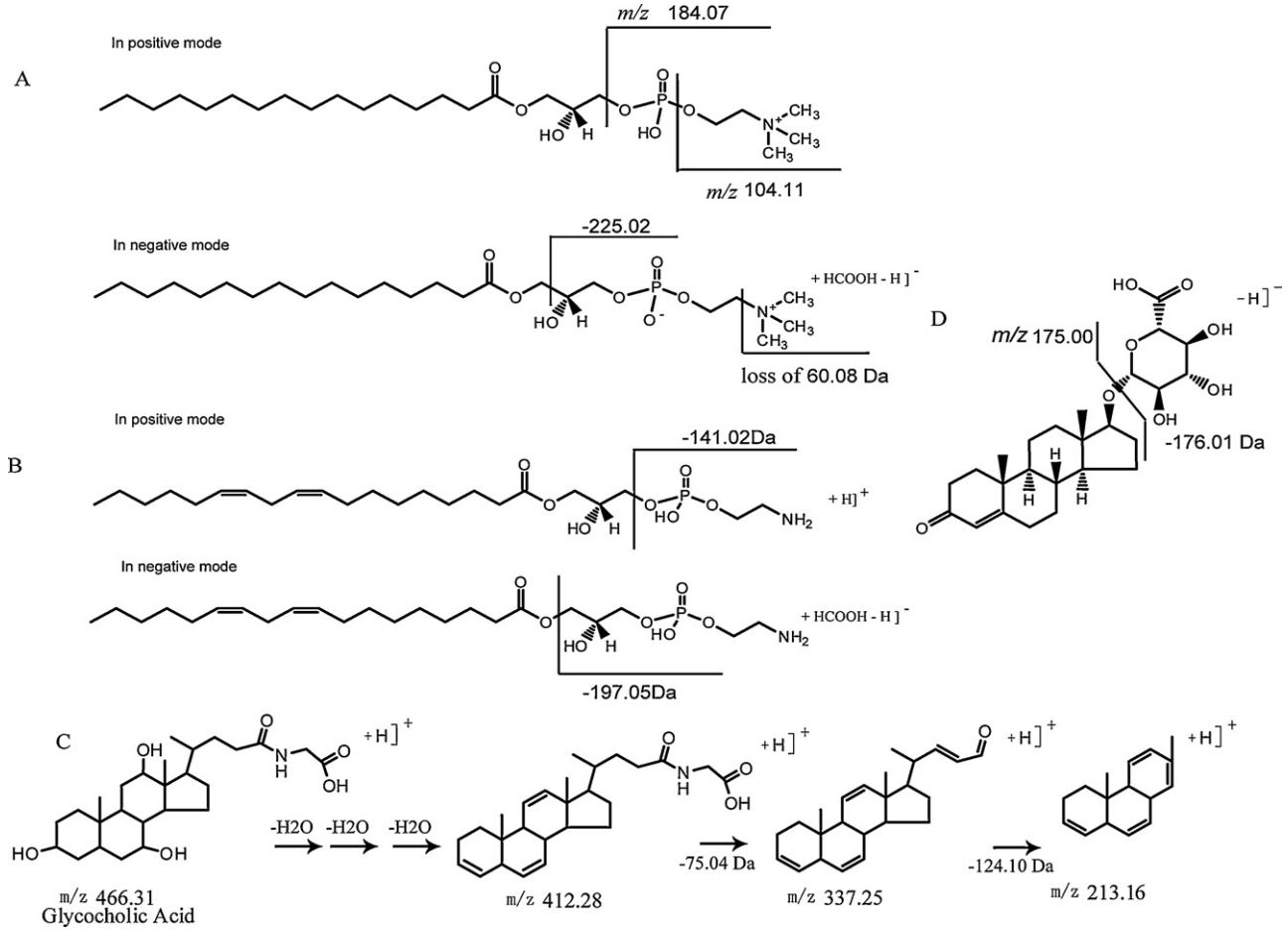

Fig. 3. (A) The characteristic fragmentation of choline glycerophospholipids, (B) ethanolamine glycerophospholipids, (C) glycine conjugates of bile acids, and (D) steroid glucuronides.

Table 1
Detection of glycerophospholipids by product ion and neutral loss filtration methods.

Peak no.	*m/z*	t_R (min)	Ion species	Formula	ppm	Assignment
1	468.3076	17.1	$[M+H]^+$	$C_{22}H_{46}NO_7P$	−1.9	LysoPC(14:0)
2	542.3239	17.7	$[M+H]^+$	$C_{28}H_{48}NO_7P$	−0.4	LysoPC(20:5)
3	468.3078	17.8	$[M+H]^+$	$C_{22}H_{46}NO_7P$	−1.4	LysoPC(14:0)
4	518.3222	18.1	$[M+H]^+$	$C_{26}H_{48}NO_7P$	−3.7	LysoPC(18:3)
5	494.3235	18.2	[M+H]+	$C_{24}H_{48}NO_7P$	−1.3	LysoPC(16:1)
6	542.3238	18.3	$[M+H]^+$	$C_{28}H_{48}NO_7P$	−0.6	LysoPC(20:5)
7	518.3228	18.5	$[M+H]^+$	$C_{26}H_{48}NO_7P$	−2.5	LysoPC(18:3)
8	494.3243	18.9	$[M+H]^+$	$C_{24}H_{48}NO_7P$	0.4	LysoPC(16:1)
9	520.3398	19.7	$[M+H]^+$	$C_{26}H_{50}NO_7P$	0.1	LysoPC(18:2)
10	542.324	19.7	$[M+H]^+$	$C_{28}H_{48}NO_7P$	−0.2	LysoPC(20:5)
11	568.3387	19.7	$[M+H]^+$	$C_{28}H_{50}NO_7P$	−1.9	LysoPC(22:6)
12	544.3397	19.8	$[M+H]^+$	$C_{28}H_{50}NO_7P$	−0.1	LysoPC(20:4)
13	568.3395	20.3	$[M+H]^+$	$C_{28}H_{50}NO_7P$	−0.5	LysoPC(22:6)
14	520.3399	20.5	$[M+H]^+$	$C_{26}H_{50}NO_7P$	0.3	LysoPC(18:2)
15	544.3395	20.5	$[M+H]^+$	$C_{28}H_{50}NO_7P$	−0.5	LysoPC(20:4)
16	542.3247	20.6	$[M+H]^+$	$C_{28}H_{48}NO_7P$	1.1	LysoPC(20:5)
17	570.3562	20.9	$[M+H]^+$	$C_{30}H_{52}NO_7P$	1.4	LysoPC(22:5)
18	496.3398	21.4	$[M+H]^+$	$C_{24}H_{50}NO_7P$	0.1	LysoPC(16:0)
19	518.3241	21.5	$[M+H]^+$	$C_{26}H_{48}NO_7P$	−1.6	LysoPC(18:3)
20	570.3561	21.7	$[M+H]^+$	$C_{30}H_{52}NO_7P$	1.0	LysoPC(22:5)
21	496.3421	22.4	$[M+H]^+$	$C_{24}H_{50}NO_7P$	0.5	LysoPC(16:0)
22	546.3518	22.4	$[M+H]^+$	$C_{28}H_{52}NO_7P$	−6.6	LysoPC(20:3)
23	518.3243	22.8	$[M+H]^+$	$C_{26}H_{48}NO_7P$	0.4	LysoPC(18:3)
24	546.3523	22.8	$[M+H]^+$	$C_{28}H_{52}NO_7P$	−5.7	LysoPC(20:3)
25	522.3548	23.1	$[M+H]^+$	$C_{26}H_{52}NO_7P$	−1.2	LysoPC(18:1)
26	570.3555	23.1	$[M+H]^+$	$C_{30}H_{52}NO_7P$	0.1	LysoPC(22:5)
27	522.3554	24.2	$[M+H]^+$	$C_{26}H_{52}NO_7P$	0.0	LysoPC(18:1)
28	510.3544	24.6	$[M+H]^+$	$C_{25}H_{52}NO_7P$	−2.1	LysoPC(17:0)
29	548.3711	24.7	$[M+H]^+$	$C_{28}H_{54}NO_7P$	−2.3	LysoPC(20:2)
30	510.3552	25.8	$[M+H]^+$	$C_{25}H_{52}NO_7P$	−0.4	LysoPC(17:0)
31	548.3707	25.9	$[M+H]^+$	$C_{28}H_{54}NO_7P$	−0.7	LysoPC(20:2)
32	550.3819	25.9	$[M+H]^+$	$C_{28}H_{56}NO_7P$	−2.9	LysoPC(20:1)
33	508.3761	26.3	$[M+H]^+$	$C_{26}H_{54}NO_6P$	−0.1	LysoPC(O-18:1)
34	482.3240	26.8	$[M+H]^+$	$C_{23}H_{48}NO_7P$	−0.2	LysoPC(15:0)
35	524.3711	27.9	$[M+H]^+$	$C_{26}H_{54}NO_7P$	−0.1	LysoPC(18:0)
36	546.3517	27.9	$[M+H]^+$	$C_{28}H_{52}NO_7P$	−6.8	LysoPC(20:3)
37	482.3228	28.1	$[M+H]^+$	$C_{23}H_{48}NO_7P$	−2.7	LysoPC(15:0)
38	546.3554	28.4	$[M+H]^+$	$C_{28}H_{52}NO_7P$	−2.6	LysoPC(20:3)
39	546.3554	29.3	$[M+H]^+$	$C_{28}H_{52}NO_7P$	−2.6	LysoPC(20:3)
40	524.3711	29.3	$[M+H]^+$	$C_{26}H_{54}NO_7P$	0.1	LysoPC(18:0)
41	550.3857	29.2	$[M+H]^+$	$C_{28}H_{56}NO_7P$	−1.9	LysoPC(20:1)
42	482.3227	19.1	$[M+H]^+$	$C_{23}H_{48}NO_7P$	−2.9	LysoPE(18:0)
43	478.2917	19.3	$[M+H]^+$	$C_{23}H_{44}NO_7P$	−2.3	LysoPE(18:2)
44	502.2920	19.5	$[M+H]^+$	$C_{25}H_{44}NO_7P$	−1.6	LysoPE(20:4)
45	482.3227	19.9	$[M+H]^+$	$C_{23}H_{48}NO_7P$	−2.9	LysoPE(18:0)
46	478.2919	20.2	$[M+H]^+$	$C_{23}H_{44}NO_7P$	−1.9	LysoPE(18:2)
47	502.2919	20.1	$[M+H]^+$	$C_{25}H_{44}NO_7P$	−1.8	LysoPE(20:4)
48	454.2913	20.9	$[M+H]^+$	$C_{21}H_{44}NO_7P$	−3.3	LysoPE(16:0)
49	454.2922	21.8	$[M+H]^+$	$C_{21}H_{44}NO_7P$	−1.4	LysoPE(16:0)

PC, Lyso PC; PE, Lyso PE.

be determined by high energy CID [20]. However, (ESI)MS-Q-TOF in routine use do not generate collisions in the keV ranges which were required to produce products of fatty acyls. Additionally, the high energy CID spectra often exhibited the abundant $[M-H-H_2O]^-$, $[M-H-2H_2O]^-$, $[M-H-H_2O-CO_2]^-$, and $[M-H-2H_2O-CO_2]^-$ ions and skillful data interpretation was needed in pursuing the analysis [7]. To address this problem, we introduced the mass defect filtration.

The standard mass defect profile was depicted by more than 600 protonated fatty acyl molecules, which included straight chain fatty acids, branched fatty acids, octadecanoids, eicosanoids, docosanoids. Fig. 5A demonstrated the coincidence plot of the measured ions (expressed as the black dots) and the extract ions of published fatty acyls (expressed as the white dots). From the profile, although the standard mass defect value spanned to 0.8000, the overlapped region ranged from 100 to 500 in *x-axis* and from 0.000 to 0.4000 in *y-axis*. The mass defect tolerance was correspondingly determined as ±200 mDa and the central formula was determined as $C_{14}H_{27}O$ and the mass defect filtration was correspondingly set at ($C_{14}H_{27}O \pm 200$ mDa). The filtered chromatogram was shown in Fig. 6B and 432 of 4561 spectra were obtained. It was indicated that roughly 89.2% spectra were excluded. With the analysis of EICs and database search, the majority of isotope ions were excluded and a total of 41 compounds were detected (Table 3).

Bile acids and derivatives were mainly detected as $[M-H]^-$ in the negative mode by analyzing the standard compounds of cholic acid, chenodeoxycholic acid, deoxycholic acid, lithocholic acid, and dehydrocholic acid. All the published unconjugated bile acids from LIPID MAP were converted into their protonated form to depict the standard mass defect profile. As demonstrated in the profile (Fig. 5B), the mass defect range was from 0.2016 ($C_{24}H_{29}O_5^-$) to 0.3578 ($C_{27}H_{47}O_2^-$) and the nominal mass range was from *m/z* 350 to *m/z* 470. By calculation, the mass defect tolerance was determined as ±78 mDa and the central formula was $C_{25.5}H_{38}O_{3.5}$. When such filtration settings as ($C_{25.5}H_{38}O_{5.5} \pm 78$ mDa) were applied in the TIC and original data, the chromatogram was greatly simplified and the complexity of spectra was reduced. As illustrated in filtered chromatogram (Fig. 6C), the noise level was greatly decreased and

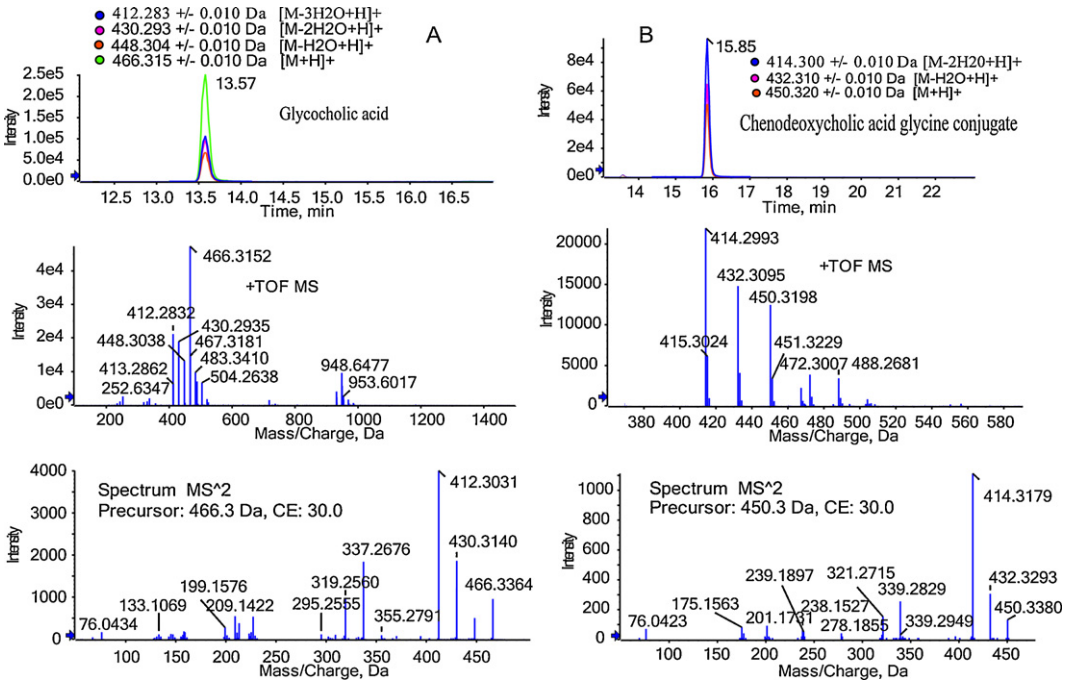

Fig. 4. The EICs and MS spectra of (A) glycocholic acid and (B) chenodeoxycholic acid glycine.

many heterogeneous peaks were ruled out with the retention time between 25 and 60 min. It was notable that 362 spectra including isotopes and adducts were screened out from original 4561 spectra. Although lots of ions were still retained, 92.1% spectra were filtered out. Further, we excluded the even nominal mass of *m*/*z* according to Nitrogen rule and only 213 spectra (including isotopic and adduct ions) was remained. By analyzing the EICs and searching database, 19 of 28 peaks were structurally identified as the potential bile acids

Table 2
Detection of glycine conjugated bile acids and glucuronide conjugated steroids by product ion and neutral loss filtration methods.

Peak no.	*m*/*z*	t_R (min)	Ion species	Formula	ppm	Assignment
50	466.3156	12.1	$[M+H]^+$	$C_{26}H_{43}NO_6$	−1.5	G-BA
51	466.3146	12.2	$[M+H]^+$	$C_{26}H_{43}NO_6$	−3.7	G-BA
52	464.2991	12.4	$[M+H]^+$	$C_{26}H_{41}NO_6$	−3.4	G-BA
53	464.2999	12.6	$[M+H]^+$	$C_{26}H_{41}NO_6$	−1.6	G-BA
54	464.2988	12.8	$[M+H]^+$	$C_{26}H_{41}NO_6$	−4.0	G-BA
55	450.3212	13.3	$[M+H]^+$	$C_{26}H_{43}NO_5$	−0.4	G-BA
56	450.3196	13.7	$[M+H]^+$	$C_{26}H_{43}NO_5$	−4.0	G-BA
57	466.3153	13.7	$[M+H]^+$	$C_{26}H_{43}NO_6$	−2.2	G-BA
58	432.3108	14.7	$[M+H]^+$	$C_{26}H_{41}NO_4$	−2.9	G-BA
59	450.3201	16.0	$[M+H]^+$	$C_{26}H_{43}NO_5$	−2.9	G-BA
60	450.3198	16.5	$[M+H]^+$	$C_{26}H_{43}NO_5$	−3.6	G-BA
61	417.1191	11.7	$[M-H]^-$	$C_{21}H_{21}O_9$	0.0	GlcU
62	417.1181	12.2	$[M-H]^-$	$C_{21}H_{21}O_9$	−0.7	GlcU
63	389.1250	12.6	$[M-H]^-$	$C_{20}H_{21}O_8$	2.1	GlcU
64	473.1460	12.6	$[M-H]^-$	$C_{24}H_{25}O_{10}$	1.4	GlcU
65	389.1242	12.8	$[M-H]^-$	$C_{20}H_{21}O_8$	0.0	GlcU
66	433.1135	12.8	$[M-H]^-$	$C_{21}H_{20}O_{10}$	−1.2	GlcU
67	473.1455	12.8	$[M-H]^-$	$C_{24}H_{25}O_{10}$	0.4	GlcU
68	433.1142	13.0	$[M-H]^-$	$C_{21}H_{20}O_{10}$	0.4	GlcU
69	387.1090	13.1	$[M-H]^-$	$C_{20}H_{20}O_8$	1.2	GlcU
70	507.2233	13.1	$[M-H]^-$	$C_{26}H_{35}O_{10}$	−0.5	GlcU
71	433.1152	13.2	$[M-H]^-$	$C_{21}H_{20}O_{10}$	2.7	GlcU
72	387.1080	13.3	$[M-H]^-$	$C_{20}H_{20}O_8$	−1.4	GlcU
73	509.2399	13.3	$[M-H]^-$	$C_{26}H_{37}O_{10}$	1.3	GlcU
74	509.2395	13.3	$[M-H]^-$	$C_{26}H_{37}O_{10}$	0.5	GlcU
75	389.1247	13.6	$[M-H]^-$	$C_{20}H_{21}O_8$	1.3	GlcU
76	389.1247	13.8	$[M-H]^-$	$C_{20}H_{21}O_8$	1.3	GlcU
77	509.2392	13.9	$[M-H]^-$	$C_{26}H_{37}O_{10}$	0.0	GlcU
78	387.1091	14.0	$[M-H]^-$	$C_{20}H_{20}O_8$	1.4	GlcU
79	401.1247	14.5	$[M-H]^-$	$C_{21}H_{21}O_8$	1.3	GlcU
80	491.2288	15.1	$[M-H]^-$	$C_{26}H_{35}O_9$	0.3	GlcU
81	401.1252	15.2	$[M-H]^-$	$C_{21}H_{21}O_8$	2.5	GlcU
82	493.2247	16.0	$[M-H]^-$	$C_{26}H_{37}O_9$	0.8	GlcU
83	493.2248	16.5	$[M-H]^-$	$C_{26}H_{37}O_9$	1.0	GlcU
84	493.2450	17.7	$[M-H]^-$	$C_{26}H_{37}O_9$	1.4	GlcU

G-BA, glycine conjugates of bile acids; GlcU, glucuronide conjugated steroids.

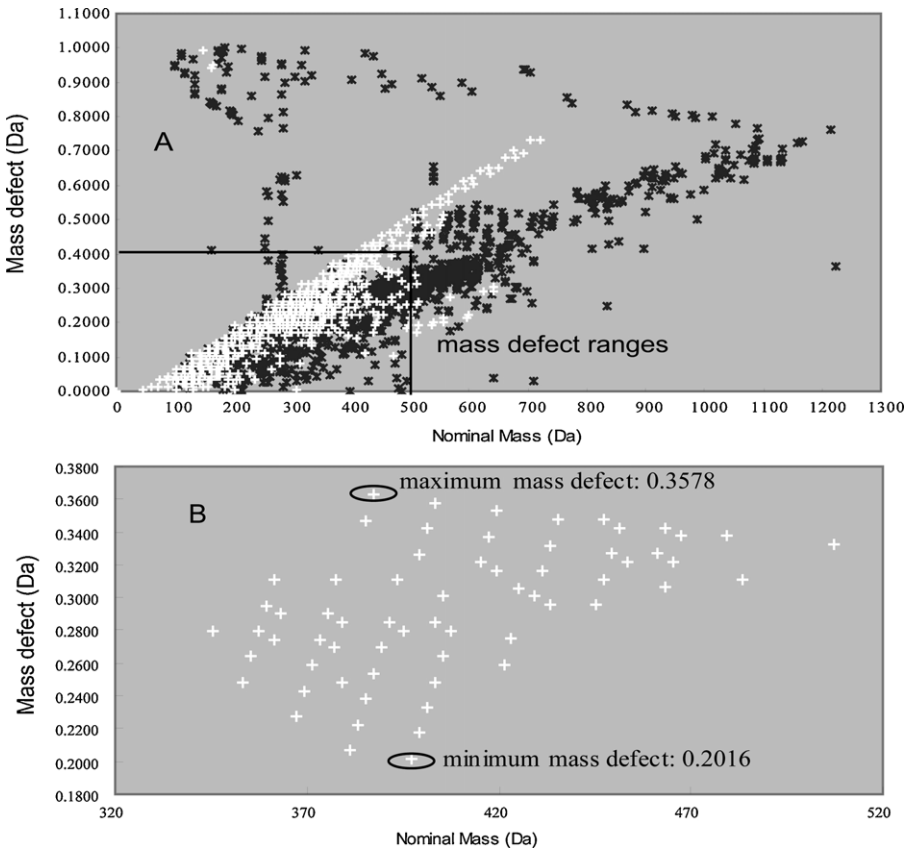

Fig. 5. (A) The coincidence plots of the detected ions (expressed as the black dots) in the analytical sample and the published fatty acyls (expressed as the white dots) and (B) the standard mass defect plots of bile acids, the maximum mass defect value was 0.3578 ($C_{24}H_{29}O_5$) and the minimum mass defect value was 0.2016 ($C_{27}H_{47}O_2$).

and their derivatives (Table 4). The false positive compounds were identified as sterol compounds and fatty acyls. These molecules possess similar mass defect profile with bile acids and derivatives. Although the accuracy of detection was 67.85%, the false candidates were retrieved from the database searching and MS/MS matching.

3.3. Method validation of quantitative analysis

Methodological validation was conducted by all the detected peaks both in the positive and negative ion modes to investigate the quantitative performance. The responses were normalized to the two internal compounds. Rheinic acid was used for negative ionization calibration and diazepam was used for positive ionization calibration.

Linearity: Because lipids are endogenous compounds widely presenting in the mammalian plasma, and tissues, the blank matrix and the standard compounds are always inaccessible. Several studies spiked the representative pure compounds into plasma to prepare the calibration and the linearity was calculated by subtracting the nonspiked samples from spiked samples [23]. This approach could not reflect all the detected molecules. In our study, the "diluted calibration curves" was used to construct the calibration curves which were described previously by our laboratory [24]. The "diluted calibration curves" was prepared by sequentially diluting the 200 μL rat plasma with normal saline to achieve the final volumetric concentration at 3.125, 6.25, 12.5, 25, 50, 100, and 200 μL/200 μL. Then, calibration curves were constructed by plotting the peak area ratios (analysts/internal standards) against the volumetric concentrations with weighted linear regression (weighing factor: $1/x$). The results of five batches (Supplementary information, Tables S1–S3) demonstrated that sufficient dynamic ranges with the correlation coefficients (R^2) exceeding 0.99 was obtained for all the detected lipids and the accuracy, expressed as relative errors (RE%), was lower than ±15%.

Precision and accuracy: The precision and accuracy was assessed by the intra- and inter-day variations. The intra-day variations were analyzed by the three replicates at the volumetric concentration 100 μL/200 μL in one day. The inter-day variations were analyzed by the three replicates at the volumetric concentration 100 μL/200 μL over three consecutive days. The obtained results (Supplementary information, Tables S1–S3) suggested that, the relative standard deviation (RSD) values of intra-day and inter-day variation were within ±15%.

3.4. Application

We applied our approach for the biological samples from the rats fed with high-fat diet, energy-restricted diet and normal diet to identify diet specific lipid features. We pooled equal aliquots from the three groups to prepare the quality control samples and analyzed quality control samples at the start of each batch in the whole analysis to check the analytical variability. The principal component analysis (PCA) model was conducted and a good three principal components mode was generated, which explained 66.9% and predicted 92.6% of the variables ($R^2X = 0.689$ and $Q^2 = 0.625$). From the 2D score plot for the first and the second principal component (Supplementary information, Fig. S1), there was a clear separation between the quality control samples and the other groups, supporting a reliable analysis with our method. The repeatability by peak area was also examined and the obtained variation was found to be acceptable with the RSD values ranging from 0.5% to 16.67%.

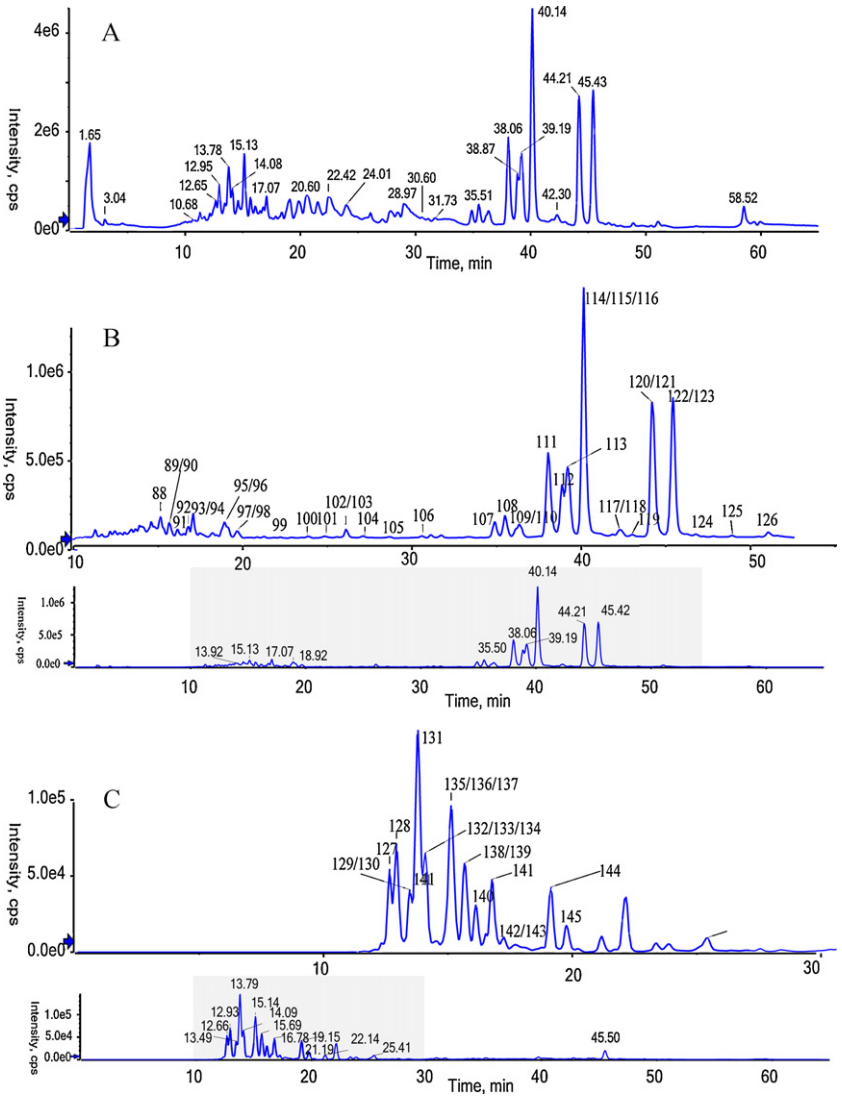

Fig. 6. (A) The unfiltered chromatogram determined in negative ion mode and the filtered chromatograms of (B) fatty acyls and (C) unconjugated bile acids obtained by product ion or mass defect filtration method.

The systematic lipid analysis of the different groups was conducted by a PCA model ($R^2X = 0.708$ and $Q^2 = 0.442$). Fig. 7A described the score plot for the first and the second principal components, which clearly showed that the lipids of the high fat diet fed rats were separated from the other two groups by the first principal component. From the corresponding loadings plot (Fig. 7B), a significant number of the variables were located around the observations of the high-fat diet fed rats, indicating that the lipid profile

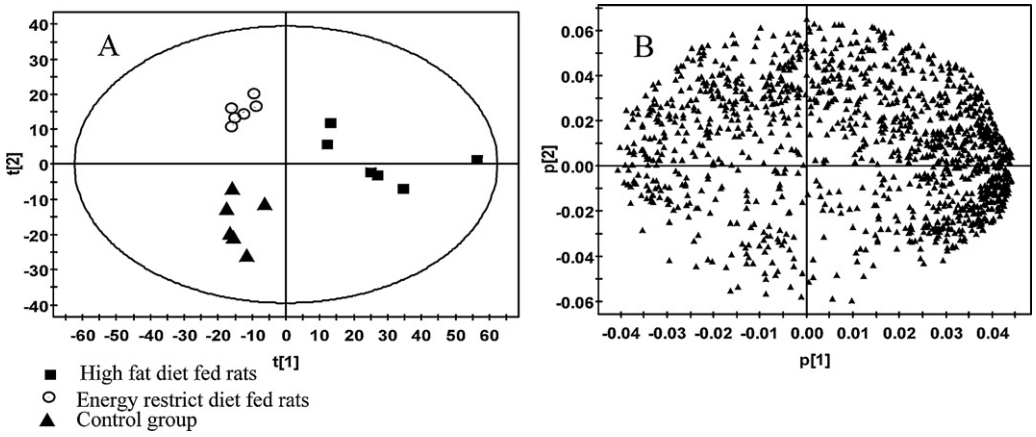

Fig. 7. (A) The score plot of all observations and (B) the corresponding loading plot of three groups in the PCA model excluding quality control samples.

Table 3
Detection of fatty acids and unconjugated bile acids by mass defect filtration method.

Peak no.	*m/z*	t_R (min)	Ion species	Formula	ppm	Assignment
85	331.1920	12.2	$[M-H]^-$	$C_{20}H_{28}O_4$	1.6	Eic
86	331.1921	13.7	$[M-H]^-$	$C_{20}H_{28}O_4$	1.9	Eic
87	333.2077	14.4	$[M-H]^-$	$C_{20}H_{30}O_4$	1.7	Eic
88	335.2228	15.1	$[M-H]^-$	$C_{20}H_{32}O_4$	0.0	Eic
89	331.1918	16.0	$[M-H]^-$	$C_{20}H_{28}O_4$	1.0	Eic
90	257.1760	16.5	$[M-H]^-$	$C_{14}H_{26}O_4$	0.6	FA
91	315.1971	16.9	$[M-H]^-$	$C_{20}H_{28}O_3$	1.7	Eic
92	333.2076	17.9	$[M-H]^-$	$C_{20}H_{30}O_4$	1.4	Eic
93	313.2388	18.2	$[M-H]^-$	$C_{18}H_{34}O_4$	1.2	FA
94	333.2076	18.3	$[M-H]^-$	$C_{20}H_{30}O_4$	1.4	Eic
95	335.2234	18.5	$[M-H]^-$	$C_{20}H_{32}O_4$	1.8	Eic
96	317.2125	18.7	$[M-H]^-$	$C_{20}H_{30}O_3$	0.9	Eic
97	315.1974	19.5	$[M-H]^-$	$C_{20}H_{28}O_3$	2.6	Eic
98	315.1971	20.1	$[M-H]^-$	$C_{20}H_{28}O_3$	1.7	Eic
99	311.2237	22.6	$[M-H]^-$	$C_{18}H_{32}O_4$	2.9	FA
100	295.2288	23.6	$[M-H]^-$	$C_{18}H_{32}O_3$	3.2	FA
101	343.2285	25.3	$[M-H]^-$	$C_{22}H_{32}O_3$	1.8	Doc
102	295.2285	25.6	$[M-H]^-$	$C_{18}H_{32}O_3$	2.1	FA
103	319.2288	25.8	$[M-H]^-$	$C_{20}H_{32}O_3$	2.9	Eic
104	295.2287	27.5	$[M-H]^-$	$C_{18}H_{32}O_3$	2.8	FA
105	295.2285	28.4	$[M-H]^-$	$C_{18}H_{32}O_3$	2.1	FA
106	275.2021	31.4	$[M-H]^-$	$C_{18}H_{28}O_2$	1.6	FA
107	301.2177	34.5	$[M-H]^-$	$C_{20}H_{30}O_2$	1.3	FA
108	227.2022	36.0	$[M-H]^-$	$C_{14}H_{28}O_2$	2.4	FA
109	253.2178	37.7	$[M-H]^-$	$C_{16}H_{30}O_2$	2.0	FA
110	327.2336	37.7	$[M-H]^-$	$C_{20}H_{32}O_2$	2.0	FA
111	303.2336	38.8	$[M-H]^-$	$C_{20}H_{32}O_2$	2.1	FA
112	305.2494	39.1	$[M-H]^-$	$C_{20}H_{34}O_2$	2.6	FA
113	279.2340	39.2	$[M-H]^-$	$C_{18}H_{32}O_2$	3.7	FA
114	329.2492	40.0	$[M-H]^-$	$C_{22}H_{34}O_2$	1.8	FA
115	267.2336	41.4	$[M-H]^-$	$C_{17}H_{32}O_2$	2.4	FA
116	329.2494	41.8	$[M-H]^-$	$C_{22}H_{34}O_2$	2.4	FA
117	305.2495	42.0	$[M-H]^-$	$C_{20}H_{34}O_2$	2.9	FA
118	305.2493	42.6	$[M-H]^-$	$C_{20}H_{34}O_2$	2.3	FA
119	255.2337	43.1	$[M-H]^-$	$C_{16}H_{32}O_2$	2.9	FA
120	255.2337	43.8	$[M-H]^-$	$C_{16}H_{32}O_2$	2.9	FA
121	331.2651	44.2	$[M-H]^-$	$C_{22}H_{36}O_2$	2.6	FA
122	281.2494	45.0	$[M-H]^-$	$C_{18}H_{34}O_2$	2.8	FA
123	269.2494	46.2	$[M-H]^-$	$C_{17}H_{32}O_2$	3.0	FA
124	307.2653	46.4	$[M-H]^-$	$C_{20}H_{36}O_2$	3.4	FA
125	269.2494	47.4	$[M-H]^-$	$C_{17}H_{32}O_2$	3.0	FA
126	283.2651	50.7	$[M-H]^-$	$C_{18}H_{36}O_2$	3.0	FA

FA, fatty acids and conjugates; Doc, docosanoids; Eic, eicosanoids.

was strongly influenced. The further validation by one-way ANOVA suggested that the high fat diet increased the level of eicosanoids by two or three fold, as illustrated by peak 94, 95, and 96. It was well known that eicosanoids exerted a complex role in many physiological systems, especially in inflammation. Elevation of eicosanoids by high fat diet indicated the involvement of inflammation in high fat diet. Conversely, energy-restricted diet provoked the decrease of the fatty acyls (such as peak 107, 108, 109, and 112),

Table 4
Detection of unconjugated bile acids by mass defect filtration method.

Peak no.	*m/z*	t_R (min)	Ion species	Formula	ppm	Assignment
127	405.2652	12.7	$[M-H]^-$	$C_{24}H_{38}O_5$	1.4	BA
128	407.2803	13.0	$[M-H]^-$	$C_{24}H_{40}O_5$	0.0	BA
129	405.2651	13.4	$[M-H]^-$	$C_{24}H_{38}O_5$	1.1	BA
130	407.2803	13.5	$[M-H]^-$	$C_{24}H_{40}O_5$	0.0	BA
131	407.2803	13.7	$[M-H]^-$	$C_{24}H_{40}O_5$	0.2	BA
132	405.2655	14.0	$[M-H]^-$	$C_{24}H_{38}O_5$	2.1	BA
133	407.2803	14.1	$[M-H]^-$	$C_{24}H_{40}O_5$	0.0	BA
134	405.2652	14.6	$[M-H]^-$	$C_{24}H_{38}O_5$	1.4	BA
135	407.2802	15.1	$[M-H]^-$	$C_{24}H_{40}O_5$	−0.2	BA
136	405.2653	15.3	$[M-H]^-$	$C_{24}H_{38}O_5$	1.6	BA
137	391.2851	15.4	$[M-H]^-$	$C_{24}H_{40}O_4$	−0.7	BA
138	389.2703	15.5	$[M-H]^-$	$C_{24}H_{38}O_4$	1.5	BA
139	391.2855	15.7	$[M-H]^-$	$C_{24}H_{40}O_4$	0.3	BA
140	389.2700	16.5	$[M-H]^-$	$C_{24}H_{38}O_4$	0.7	BA
141	391.2855	16.9	$[M-H]^-$	$C_{24}H_{40}O_4$	0.3	BA
142	389.2702	17.3	$[M-H]^-$	$C_{24}H_{38}O_4$	1.2	BA
143	391.2856	17.3	$[M-H]^-$	$C_{24}H_{40}O_4$	0.6	BA
144	391.2858	19.1	$[M-H]^-$	$C_{24}H_{40}O_4$	1.1	BA
145	391.2858	19.8	$[M-H]^-$	$C_{24}H_{40}O_4$	1.1	BA

suggesting that the fatty acyls were broken down for energy supply by oxidation in energy-restricted diet. To our knowledge, there was no previous report of any clear difference among the lipid profiles of high-fat diet, energy-restricted diet, and normal diet fed rats. The results in this study confirmed the important value of potential indicators of the dietary state.

4. Conclusions

High resolution MS analysis, coupled with multiple post acquisition data processing approaches provided a flexible and powerful platform for rapid analysis of multiple lipid species. In this study, product ion, neutral loss, and mass defect filtering methods were proposed for rapid detection and identification of the individual lipid species, which increased efficiency and especially facilitated the exploration of the low abundance peaks in biological samples. It was noteworthy that mass defect based filtration enabled detection independent on fragmentation patterns, which was completely different from, but complementary to fragment ions and neutral loss filtration. However, the unambiguous structural characterization was not achievable in this study because the completed fragmentation was required to distinguish the intra-class isobaric compounds.

Acknowledgments

This study was supported by National Nature Science Fund (88102881, 30973583, and 30801422), National Key New Drug Creation Special Programme (2009ZX09304-001; 2009ZX09502-004), the Program for New Century Excellent Talents in University (NCET-09-0770), and a Foundation for the Author of National Excellent Doctoral Dissertation of PR China (Grant 200979).

Appendix A. Supplementary data

Supplementary data associated with this article can be found, in the online version, at http://dx.doi.org/10.1016/j.jchromb.2012.08.001.

References

[1] M. Yang, J. Sun, Z. Lu, G. Chen, S. Guan, X. Liu, B. Jiang, M. Ye, D.A. Guo, J. Chromatogr. A 1216 (2009) 2045.
[2] K. Wang, Z. Zhu, L. Yang, Y. Gao, W. Liu, H. Zhang, Y. Chai, Rapid Commun. Mass Spectrom. 25 (2011) 9.
[3] H.Y. Wang, X. Chu, Z.X. Zhao, X.S. He, Y.L. Guo, J. Chromatogr. B: Analyt. Technol. Biomed. Life Sci. 879 (2011) 1166.
[4] F.L. Sauvage, L.N. Gastinel, P. Marquet, J. Chromatogr. A (2012), in press.
[5] P.D. Rainville, C.L. Stumpf, J.P. Shockcor, R.S. Plumb, J.K. Nicholson, J. Proteome Res. 6 (2007) 552.
[6] P. Zhu, W. Tong, K. Alton, S. Chowdhury, Anal. Chem. 81 (2009) 5910.
[7] D.S. Myers, P.T. Ivanova, S.B. Milne, H.A. Brown, Biochim. Biophys. Acta 1811 (2011) 748.
[8] C. Xie, D. Zhong, K. Yu, X. Chen, Bioanalysis 4 (2012) 937.
[9] M. Zhu, L. Ma, D. Zhang, K. Ray, W. Zhao, W.G. Humphreys, G. Skiles, M. Sanders, H. Zhang, Drug Metab. Dispos. 34 (2006) 1722.
[10] T. Xie, Y. Liang, H. Hao, J.A.L. Xie, P. Gong, C. Dai, L. Liu, A. Kang, X. Zheng, G. Wang, J. Chromatogr. A 1227 (2012) 234.
[11] X. Han, R.W. Gross, Mass Spectrom. Rev. 24 (2005) 367.
[12] X. Han, R.W. Gross, Expert Rev. Proteomics 2 (2005) 253.
[13] X. Han, K. Yang, H. Cheng, K.N. Fikes, R.W. Gross, J. Lipid Res. 46 (2005) 1548.
[14] N. Sanchez-Avila, J.M. Mata-Granados, J. Ruiz-Jimenez, M.D. Luque de Castro, J. Chromatogr. A 1216 (2009) 6864.
[15] D.S. Wishart, D. Tzur, C. Knox, R. Eisner, A.C. Guo, N. Young, D. Cheng, K. Jewell, D. Arndt, S. Sawhney, C. Fung, L. Nikolai, M. Lewis, M.A. Coutouly, I. Forsythe, P. Tang, S. Shrivastava, K. Jeroncic, P. Stothard, G. Amegbey, D. Block, D.D. Hau, J. Wagner, J. Miniaci, M. Clements, M. Gebremedhin, N. Guo, Y. Zhang, G.E. Duggan, G.D. Macinnis, A.M. Weljie, R. Dowlatabadi, F. Bamforth, D. Clive, R. Greiner, L. Li, T. Marrie, B.D. Sykes, H.J. Vogel, L. Querengesser, Nucleic Acids Res. 35 (2007) D521.
[16] M. Sud, E. Fahy, D. Cotter, A. Brown, E.A. Dennis, C.K. Glass, A.H. Merrill Jr., R.C. Murphy, C.R. Raetz, D.W. Russell, S. Subramaniam, Nucleic Acids Res. 35 (2007) D527.
[17] K. Sandra, S. Pereira Ados, G. Vanhoenacker, F. David, P. Sandra, J. Chromatogr. A 1217 (2010) 4087.
[18] E. Fahy, S. Subramaniam, H.A. Brown, C.K. Glass, A.H. Merrill Jr., R.C. Murphy, C.R. Raetz, D.W. Russell, Y. Seyama, W. Shaw, T. Shimizu, F. Spener, G. van Meer, M.S. VanNieuwenhze, S.H. White, J.L. Witztum, E.A. Dennis, J. Lipid Res. 46 (2005) 839.
[19] Y. Alnouti, I. Csanaky, C.D. Klaassen, J. Chromatogr. B: Analyt. Technol. Biomed. Life Sci. 873 (2008) 209.
[20] W.J. Griffiths, Mass Spectrom. Rev. 22 (2003) 81.
[21] J. Huang, S.P.R. Bathena, I.L. Csanaky, Y. Alnouti, J. Pharm. Biomed. Anal. 55 (2011) 1111.
[22] F. Cuyckens, R. Hurkmans, J.M. Castro-Perez, L. Leclercq, R.J. Mortishire-Smith, Rapid Commun. Mass Spectrom. 23 (2009) 327.
[23] K. Ekroos, I.V. Chernushevich, K. Simons, A. Shevchenko, Anal. Chem. 74 (2002) 941.
[24] Y. Liang, H. Hao, A. Kang, L. Xie, T. Xie, X. Zheng, C. Dai, L. Wan, L. Sheng, G. Wang, J. Chromatogr. A 1217 (2010) 4971.